ISSN 1392 - 1207. MECHANIKA. 2011. 17(2): 178-181

Dynamic simulations regarding the influence of the load-rigidity correlation on the working accuracy of a medical Triglide parallel robot

N. R. Rat*, M. Neagoe, D. Diaconescu***, S. D. Stan******

**Transilvania University of Brasov, B-dul Eroilor No 29, 500036 Romania, E-mail: ncretescu@unitbv.ro*
***Transilvania University of Brasov, B-dul Eroilor No 29, 500036 Romania, E-mail: mneagoe@unitbv.ro*
****Transilvania University of Brasov, B-dul Eroilor No 29, 500036 Romania, E-mail: dvdiaconescu@unitbv.ro*
*****Technical University of Cluj-Napoca, Bdul Muncii, 400641 Romania, E-mail: sergiustan@ieee.ro*

crossref http://dx.doi.org/10.5755/j01.mech.17.2.336

1. Introduction

In the last three decades, parallel robots have been increasingly studied and developed from both theoretical viewpoints and practical applications, as the medical one.

Parallel robots are the structures with closed kinematic chains, composed by an end-effector (the mobile platform) with n DOF (degrees of freedom), connected to a base by two or more kinematical chains called legs (that can be a simple or a complex kinematic chains) [1-3].

For a like 3 DOF structure (Fig. 1), that is also the object of this paper, Stan et al. approached relevant kinematic and control aspects in [4, 5].

In this paper, starting from another dynamic applications [6-8] and using ADAMS simulations, the influence of the load-rigidity correlation on the dynamic response of the considered medical Triglide robot is highlighted; this approach compares two robot models (with rigid and with elastic connecting rods), taking into account adjustable load and adjustable rigidity of the rods AB (Fig. 1). The resulting conclusions are useful for the accuracy of the medical robot applications.

2. Inverse kinematical model

The 3 DOF Triglide parallel robot (Fig. 1) is composed by a base N connected at a mobile platform P_2 by 3 glide actuators NA_i; $i = 1, 2, 3$ and 3 parallelogram legs whit spherical joints (A_{i1}, A_{i2}, B_{i1}, B_{i2}).

The inverse kinematics of this structure supposes to establish the joint variable vector $\boldsymbol{q}(\boldsymbol{q}_1, \boldsymbol{q}_2, \boldsymbol{q}_3)$ of the actuators as against of the end-effector variable vector $P_2(x_p, y_p, z_p)$ of the mobile platform center against of the system Nxyz. The actuators' vector can be obtained from equations of the type (Fig. 1)

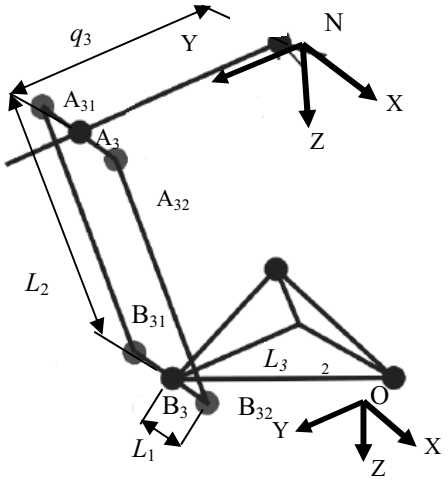

Fig. 1 Kinematic scheme of a branch from the considered medical parallel robot [9]

$$q_i^2 + q_i 2\{(x_P + L_3 \sin(\beta_i))\sin(\alpha_i) + (y_P + L_3 \cos(\beta_i))\cos(\alpha_i)\} + (x_P + L_3 \sin(\beta_i))^2 + (y_P + L_3 \cos(\beta_i))^2 + z_P^2 - L_2^2 = 0 \quad (1)$$

which α_i and $\beta_i = 0^o, 120^o, 240^o$.

This kinematical model, elaborated and simulated in [9, 10], was now extended to the rigid robot dynamic modeling.

3. Dynamic simulation using ADAMS software

For the considered medical Triglide robot (Fig. 1) [9], the influence of the load-rigidity correlation on the dynamic response is highlighted further; using ADAMS software, this approach compares two robot models (rigid robot and robot with elastic rods), with adjustable load and adjustable rigidity of the connecting rods AB.

The next prerequisites were taken into consideration:

- kinematic and dynamic modelling is made in a fixed system Oxyz whose origin O is described in the system Nxyz by vector NO (0.14 m, 0.13 m, 1.11 m);
- robot task: to describe a circle with a radius of 50 mm in a tilted plane;
- the first model of rigid robot, whose mass features are given in Table 1, is taken as reference, and the second model with elastic rods with adjustable load and adjustable rod elasticity (rods with ∅10 mm and rods with ∅20 mm) is analysed; adjustable roads' elasticity (that has the main influence) was obtained using ADAMS AutoFlex module, taking into account only the natural frequency smaller than 200 Hz for ∅10 mm and than 500 Hz for ∅20 mm;
- the material used for the elements was aluminium;
- the adjustable load is achieved by adjustable external mass: 0.5, 1.5 and 2.5 kg.

The simulations, in which the medical robot has rods with ∅10 mm and external mass of 0.5 and 1.5 kg, show that the difference between dynamic response of the rigid robot model and the response of the robot model with elastic connecting rods can be neglected; the relevant differences interfere for the mass of 2.5 kg (Figs. 2 - 7).

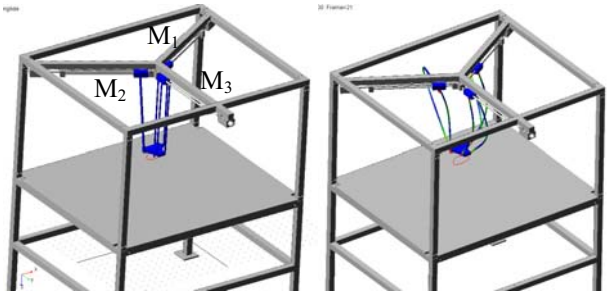

a b

Fig. 2 The 3D model of Triglide robot with rigid (a) and elastic (b) rods of ∅10 mm and external mass of 2.5 kg

Table

Mass and inertial property of all elements in movement

Rod diameter	∅10 mm	∅20 mm
$m_{tot,}$ kg	1.1604701612	3.1118806449
$J_{xx,}$ kgm^2	1.1604701612	2.1977043525
$J_{yy,}$ kgm^2	0.8136113354	2.2174092744
$J_{zz,}$ kgm^2	0.06326911582	0.1446727817
$J_{xy,}$ kgm^2	0.028778040992	0.061550150231
J_{yz} , kgm^2	0.1256409378	0.3166311606
$J_{zx,}$ kgm^2	0.1564715156	0.3837917432

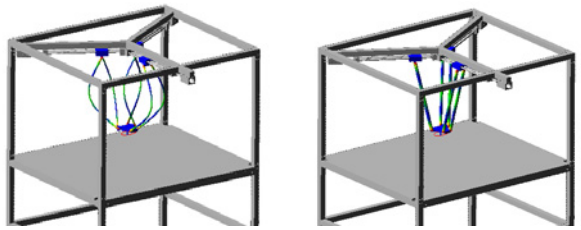

a b

Fig. 3 The 3D model of Triglide robot with elastic rods of ∅10 mm (a) and ∅20 mm (b) and external mass of 2.5 kg

The dynamic ADAMS simulations, for the case of 2.5 kg, are graphically illustrated in Figs. 3-8 and highlight the following properties.

- The displacement of the point P_2 (the centre of the mobile platform), in the case of ∅10 mm elastic roads, has a notable difference as against of rigid roads' case; this difference induces undesirable effects for speed and acceleration (Figs. 4, 5 and 6). In case of rods with ∅20 mm, the both models (rigid and elastic) give similar displacements (Fig. 4, b), with relative errors (Fig. 4, c) closed to zero (neglected errors).
- Because the responses of motors are similar, only the M3 motor response is illustrated in Figs. 7 and 8.

All displacements of the motor's are close variations (Fig. 7); this closeness can be observed also for the motor forces (Fig. 8, c), but not in the case of the elastic rods with 10 mm diameter (Fig. 8, a), in which the differences are very large; unlike the 10 mm diameter case, the 20 mm case assures a proper elasticity, for the given system, and implicitly a better response that is close to rigid case response.

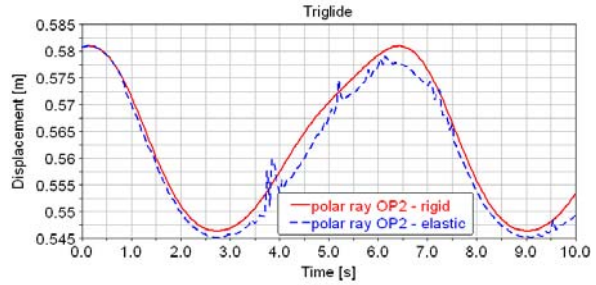

a

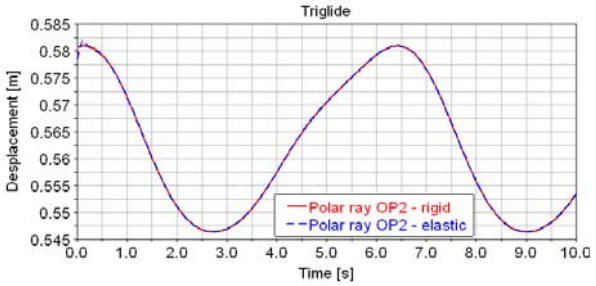

b

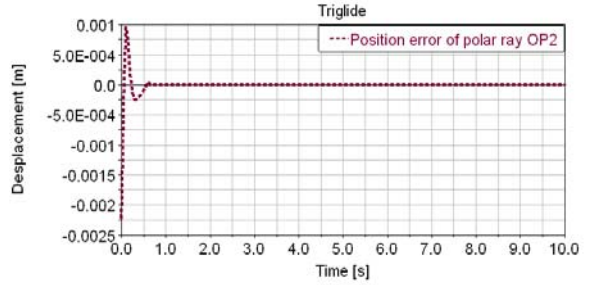

c

Fig. 4 The platform center polar-ray variation for rods with ∅10 mm (a) and with ∅20 mm (b) in the premise of rigid rods (continuous line) and elastic rods (dashed line); the difference between the polar rays afferent to the elastic model and rigid model with ∅20 mm roads (c)

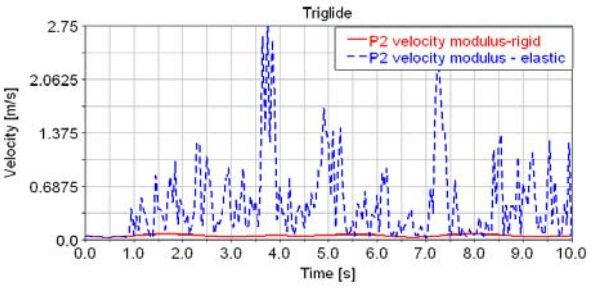

a

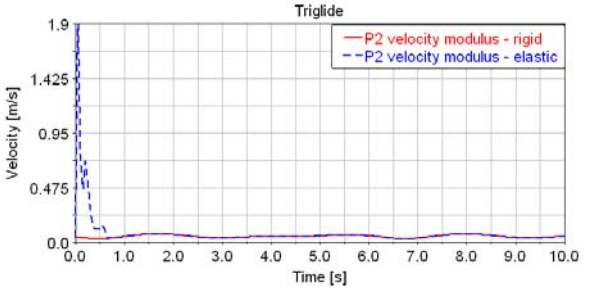

b

Fig. 5 The platform velocity variation for rods with ∅10 mm (a) and with ∅20 mm (b) in the premise of rigid rods (continuous line) and elastic rods (dashed line)

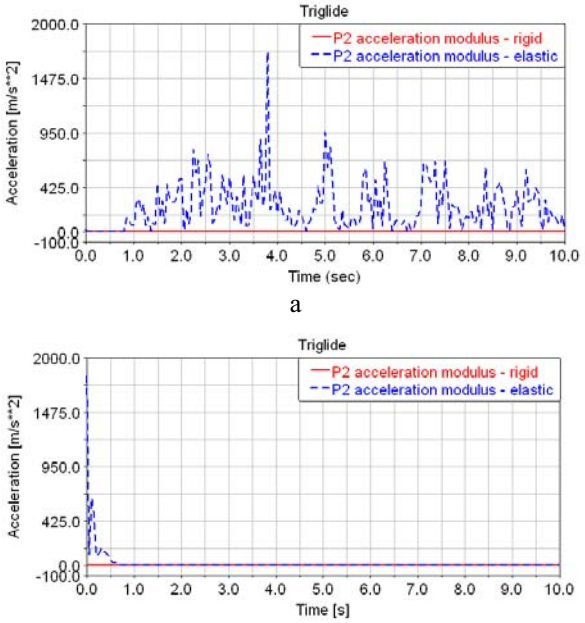

Fig. 6 The platform acceleration for rods with ∅10 mm (a) and with ∅20 mm (b) in the premise of rigid rods (continuous line) and elastic rods (dashed line)

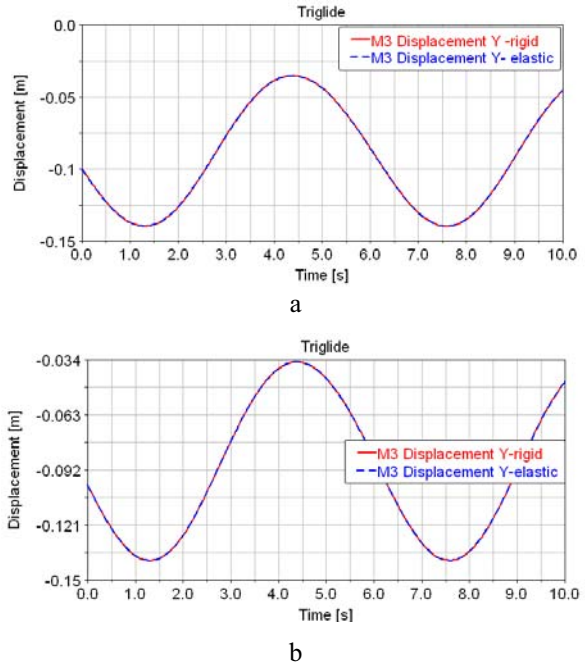

Fig. 7 Displacement variation in the M3 actuator for rigid rods (continuous line) and for elastic rods (dashed line) with ∅10 mm (a) and with ∅20 mm (b)

In the last case (with external mass of 2.5 kg), although the weight of moving elements (6 roads, 3 driving motors and the mobil platform) totalizes 3.11 kg for 20 mm roads‘ diameter (Table), unlike 1.16 kg for the 10 mm roads‘diameter, the dynamic responses of the robot with elastical elements highlight a much better working behaviour in the case with 20 mm roads‘ diameter (Fig. 3, a and b). The large elastic deformations from Fig. 2, a and Fig. 3, a, show that.

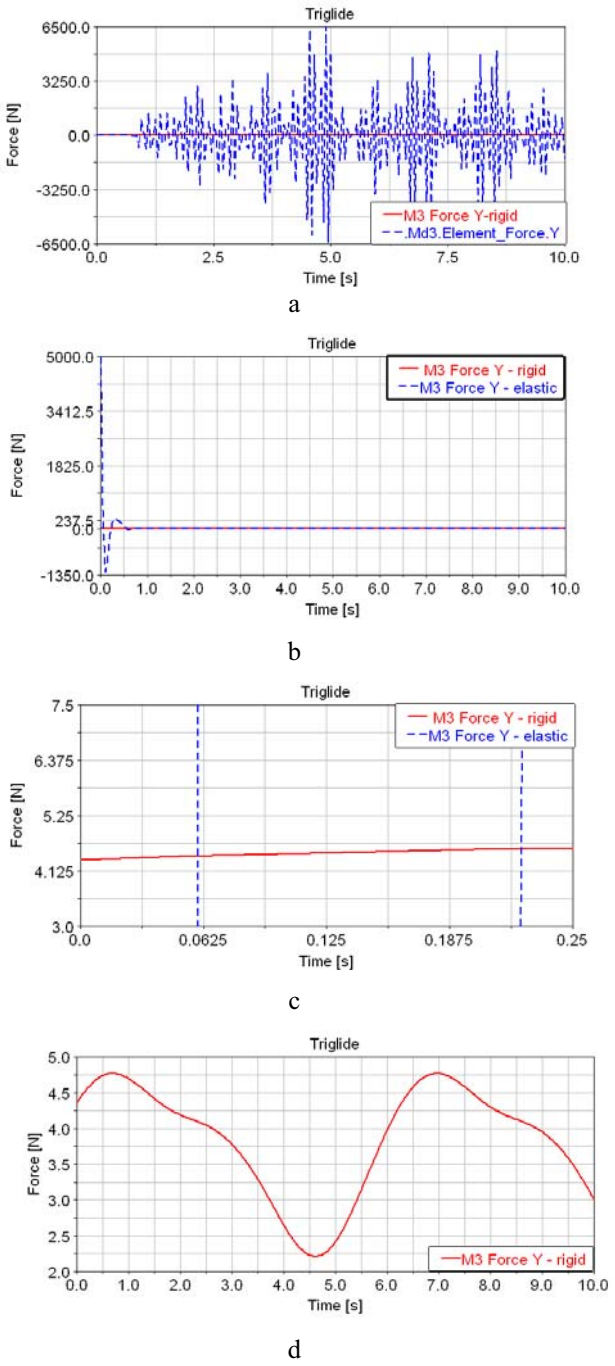

Fig. 8 Driving force variation in M3 actuator for rigid rods (continuous line) and for elastic rods (dashed line) with ∅10 mm (a) and with ∅20 mm (b); detail of b (c) and detailed force variation in the case of rigid rods with ∅20 mm (d)

4. Conclusions

1. This paper presents the dynamic analysis by ADAMS simulations (displacement, speeds, accelerations, forces and rods’ deformation), considering three values for external load (of 0.5, 1.5 and 2.5 kg) and two values for rods’ diameter (of 10 and 20 mm).

2. Te results of dynamic simulations highlight that the differences between dynamic responses of the parallel robot with rigid rods and the robot with elastic roads are negligible for the external load of 0.5 and 1.5 kg. The relevant differences interfere, the external load of 2.5 kg, be-

tween elastic model with 10 mm roads' diameter and with 20 mm roads' diameter.

3. While dynamic response of the robot with elastic roads of 20 mm diameter (and external mass of 2.5 kg) is almost the same with the rigid robot response (the proper elasticity assure a good system stability), the response of the robot with elastic roads of 10 mm diameter (and the same external mass) shows that the structure has control difficulties.

4. In accordance with the previous conclusion, a parallel robot of Triglide type can achieve a precise trajectory in medical applications, if a good correlation between roads' rigidity, external loads and robot mass is accomplished.

Acknowledgements

This work was supported by the Ministry of Education from Romania and Research grant PARTENERIATE no. 72197/1.10.2008 entitled 'Complex mechatronics systems for medical applications - SMART'.

References

1. **Gogu, G.** 2008. Structural synthesis of parallel robots. Part 1: Methodology. -Springer Verlag. 282p.
2. **Stan, S.-D. et al.** 2009. Kinematics and fuzzy control of Isoglide3 medical parallel robot, Mechanika 1(75): 62-66.
3. **Pacurari, R. et al.** 2009. Basic aspects concerning modular design of reconfigurable parallel manipulators for assembly tasks at nanoscale, Mechanika 2(76: 69-76.
4. **Stan, S.-D. et al.** 2008. Kinematics analysis, design, and control of an Isoglide3 parallel robot. The 34th IEEE, Nov. 2008, Florida: 2636-2641.
5. **Stan, S.-D. et al.** 2009. Workspace and kinematics analysis of a medical parallel robot for cardiopulmonary resuscitation. IEEE-ICIT'09, Australia: 534-539.
6. **Zhao, Y. and Gao, F.** 2009. Dynamic formulation and performance evaluation of the redundant parallel manipulator, Robotics and Computer-Integrated Manufacturing 25: 770-781.
7. **Rat, N. et al.** 2005. Comportement des robots paralleles a mouvements decouples et corps deformable. In Proc. of the 17eme Congres Français de Mecanique. Troyes, France, Act. on CD-ROM.
8. **Rat, N.R. and Neagoe, M.** Rigid vs. flexible links dynamic analysis of a 3DOF parallel robot. 3rd IEEE International Conference on Digital Ecosystems and Technologies, DEST'09, art no. 5276749: 534-539.
9. **Stan, S.-D. et al**. 2009. Kinematics analysis and design of 3DOF medical parallel robots. Springerlink book chapter, ISBN: 978-3-642-03201-1: 395-406.
10. **Stan, S.-D. et al.** 2008. Modelling, design and control of 3DOF medical parallel robot, Mechanika 6(74): 68-71.

N. R. Rat, M. Neagoe, D. Diaconescu, S. D. Stan

LYGIAGRETAUS MEDICININIO TRIJŲ SLYDIMO KINEMATINIŲ PORŲ ROBOTO DARBO TIKSLUMO KORELIACIJA ĮVERTINANT KRŪVIO PASTOVUMĄ DINAMINIO IMITAVIMO BŪDU

R ė z i u m ė

Straipsnyje pristatoma lygiagretaus medicininio trijų kinematinių slydimo porų roboto darbo tikslumo koreliacija, įvertinant krūvio pastovumą dinaminio imitavimo būdu. Parodyta, kad šis naudojamas medicinoje robotas, gali judėti tikslia trajektorija, jeigu yra pasiekta gera koreliacija tarp kelio pastovumo, išorinio krūvio ir roboto masės.

N. R. Rat, M. Neagoe, D. Diaconescu, S. D. Stan

DYNAMIC SIMULATIONS REGARDING THE INFLUENCE OF THE LOAD-RIGIDITY CORRELATION ON THE WORKING ACCURACY OF A MEDICAL TRIGLIDE PARALLEL ROBOT

S u m m a r y

The paper presents dynamic simulations regarding the influence of the load-rigidity correlation on the working accuracy of a medical Triglide parallel robot. It was proved that Triglide parallel robot can achieve a precise trajectory in medical applications, if a good correlation between roads' rigidity, external loads and robot mass is accomplished.

Н.Р. Рат, М. Неагое, Д. Диасонесцу, С.Д. Стан

КОРРЕЛЯЦИЯ ТОЧНОСТИ РАБОТЫ МЕДИЦИНСКОГО ПАРАЛЛЕЛЬНОГО РОБОТА С ТРЕМЯ КИНЕМАТИЧЕСКИМИ ПАРАМИ СКОЛЬЖЕНИЯ С УЧЕТОМ СТАБИЛЬНОСТИ НАГРУЗКИ ПРИ ДИНАМИЧЕСКОМ ИМИТИРОВАНИИ

Р е з ю м е

Статья представляет корреляцию точности работы медицинского параллельного робота с тремя кинематическими парами скольжения с учетом стабильности нагрузки при динамическом имитировании. Показано, что этот робот может осуществить точную траекторию при использовании в медицине, если достигнута хорошая корреляция между стабильностью траектории внешней нагрузки и массой робота.

Received August 02, 2010
Accepted April 05, 2011